Supplement of Geosci. Model Dev., 18, 8485–8510, 2025
https://doi.org/10.5194/gmd-18-8485-2025-supplement

Geoscientific Model Development
Open Access

Supplement of

A double-box model for aircraft exhaust plumes based on the MADE3 aerosol microphysics (MADE3 v4.0)

Monica Sharma et al.

Correspondence to: Monica Sharma (monica.sharma@dlr.de)

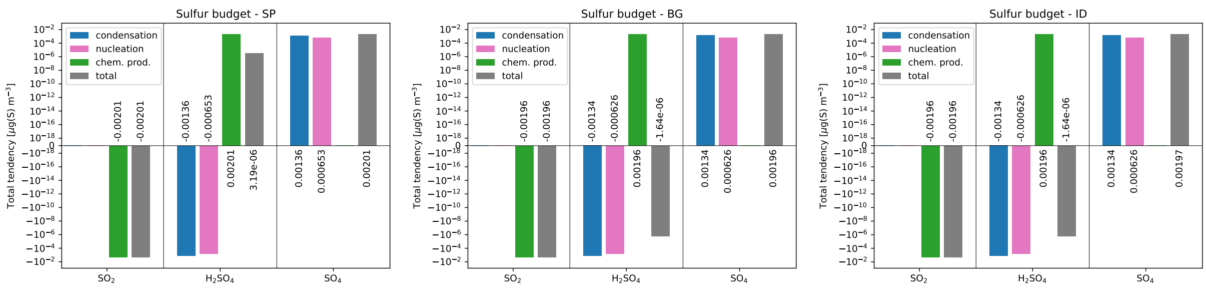

Figure S1: Analysis of the sulfur budget for the individual boxes in the plume approach (SP and BG box) and instantaneous dispersion approach (ID box) depicting the production of sulfate aerosol (SO_4) through nucleation and condensation processes in the plume model. Here, the gas-phase sulfuric acid (H_2SO_4) plays a crucial role in driving these processes. In the model, the formation of H_2SO_4 vapours is calculated online via the oxidation of sulfur dioxide (SO_2) by hydroxyl radicals (OH), which is a critical atmospheric chemical reaction.

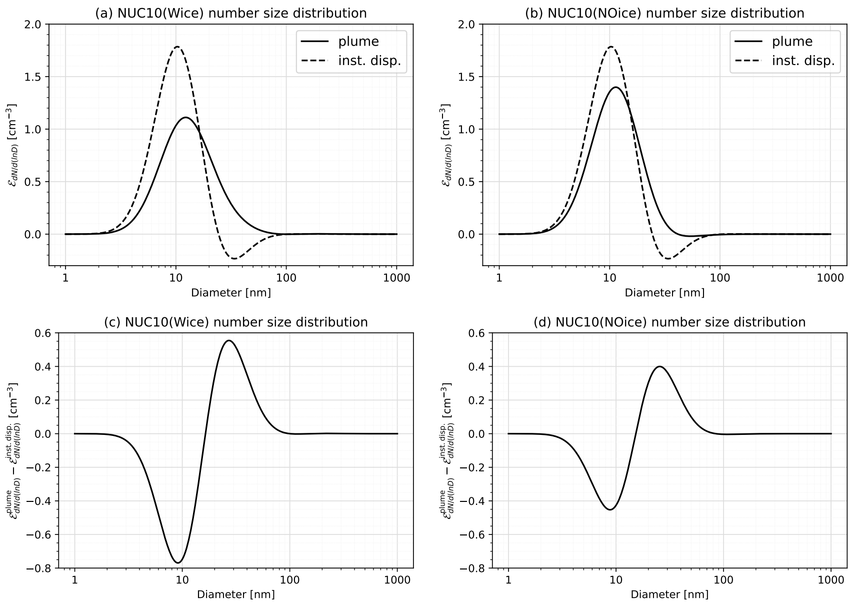

Figure S2: Aviation effect ($\mathcal{E}$) in terms of lognormal size distribution (as in Fig.7), but with the alternative assumption of 10 nm nucleation size for the newly nucleated particles. The plots represent two plume scenarios as a) NUC10(Wice) with the influence of short-lived contrail ice crystals in the vortex regime and b) NUC10(NOice) without the influence of vortex ice. Here, panels (c) and (d) show the absolute difference of the aviation effects.

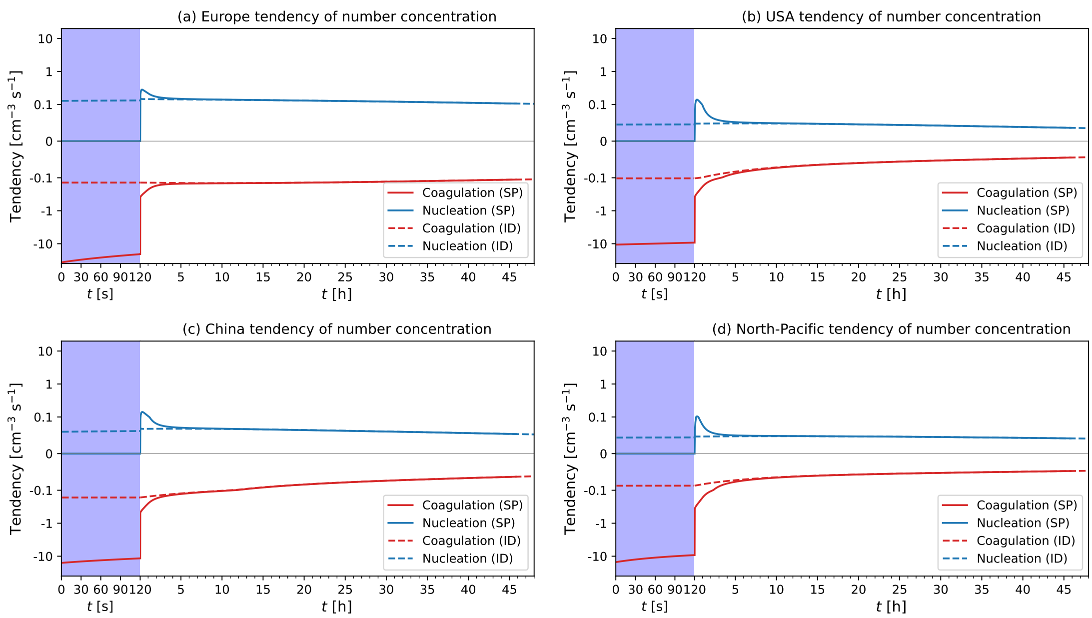

Figure S3: Tendency diagnostics performed for the aerosol number concentration in the two modelling approaches highlighting SP box (plume approach) and ID box (instantaneous dispersion approach) for the two plume regimes i.e. vortex (violet) and dispersion (white) regime. The plots illustrate two primary processes that govern aerosol number concentrations: coagulation (red) and nucleation (blue), across various regions. The regional studies specifically depict the Wice scenario only.

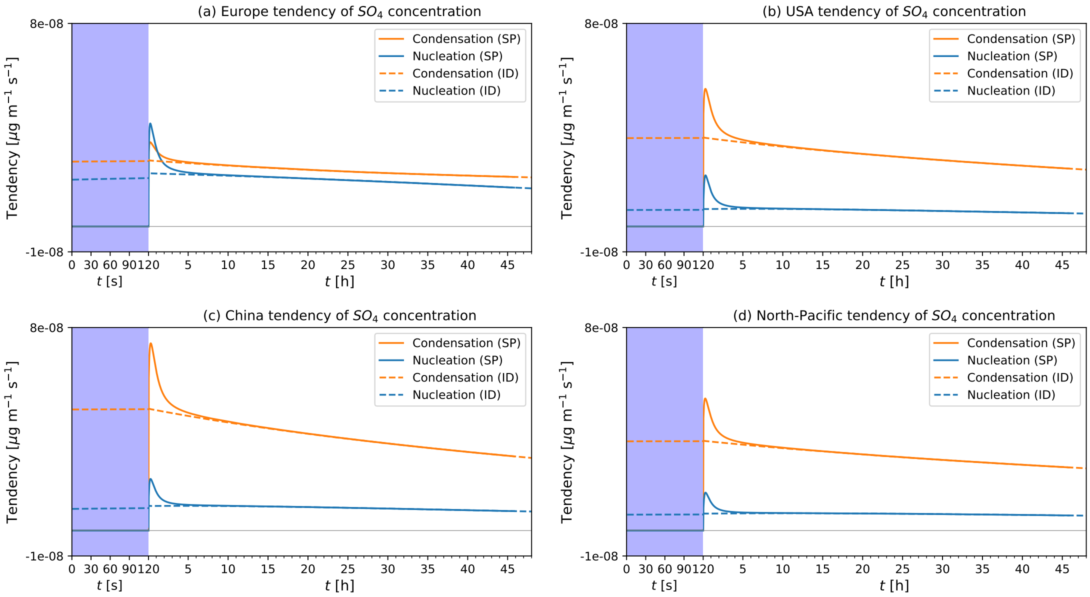

Figure S4: Tendency diagnostics performed for the SO_4 mass concentration in the two modelling approaches highlighting SP box (plume approach) and ID box (instantaneous dispersion approach) for the two plume regimes i.e. vortex (violet) and dispersion (white) regime. The plots demonstrate the two important processes involved that affects the SO_4 mass concentration in the plume model namely, condensation (orange) and nucleation (blue) across various regions. Note that the results from the regional studies specifically depict Wice scenario only.

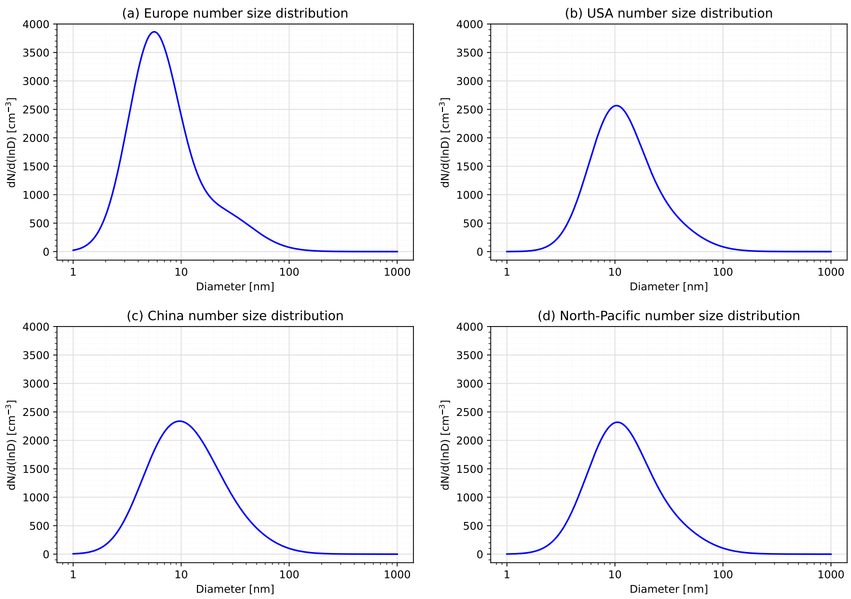

Figure S5: The plots illustrate the final size distribution in the BG box highlighting the lognormal size distribution of the aerosol particles at the reference time (t = 46 h) for various backgrounds examined in regional studies: a) Europe, b) USA, c) China and d) North-Pacific.

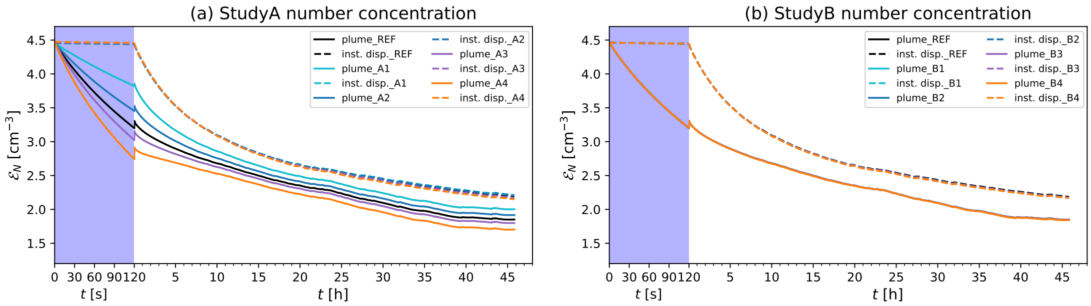

Figure S6: Aviation effect ($\mathcal{E}$) for aerosol number concentration in the two modelling approaches: plume approach (solid) and instantaneous dispersion (dashed) demonstrating the impact of study A (N_{ice}) and study B (initial soot size). The plots illustrate the variation in aerosol number concentrations in response to modifications in parameters of Study A and Study B. Here, the black line represent the reference value.

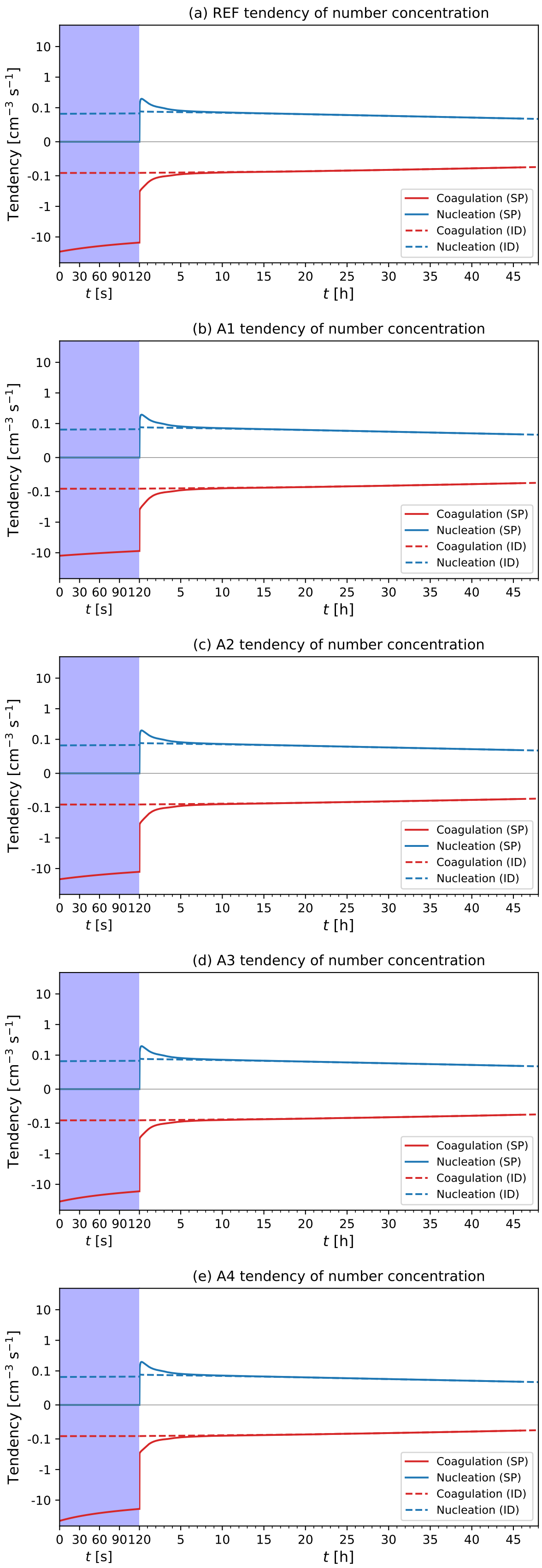

Figure S7: Tendency diagnostics as in Fig. S3, but for the parametric study A, demonstrating the modifications in the microphysical processes that influence the aerosol number concentrations in the plume model i.e. coagulation (red) and nucleation (blue), in response to altering the values of N_{ice}.

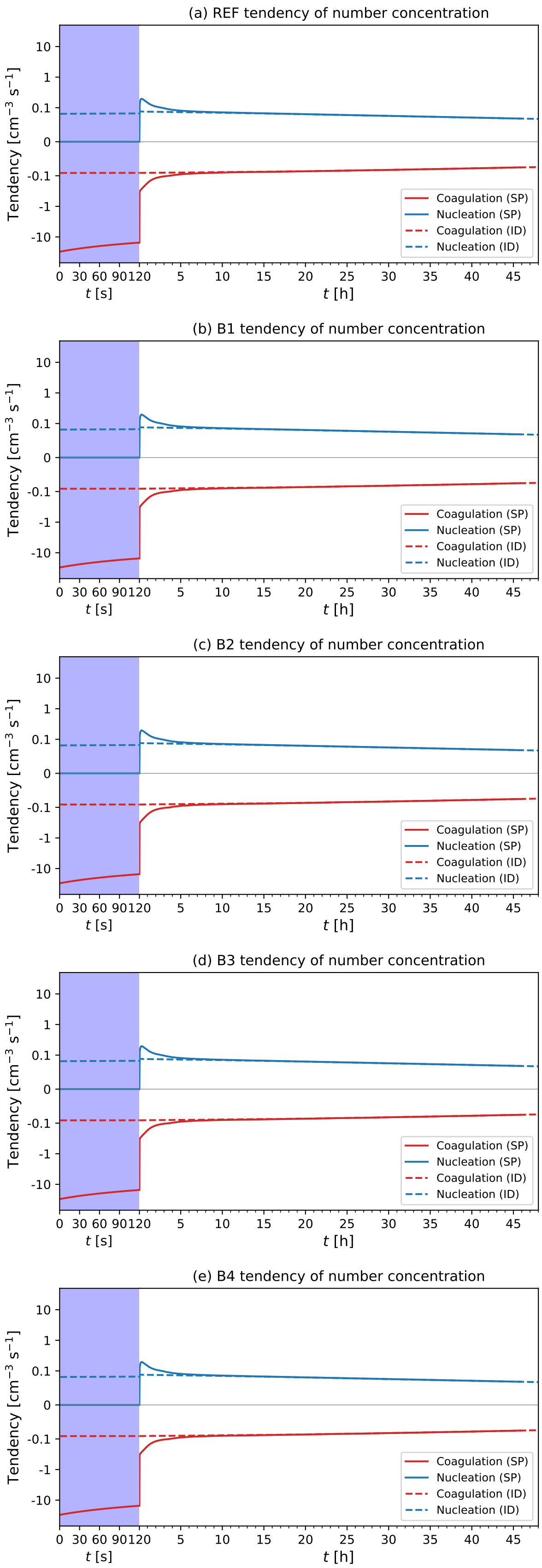

Figure S8: Tendency diagnostics as in Fig. S7, but for the parametric study B, demonstrating the modifications in the microphysical processes in response to altering the initial soot size.

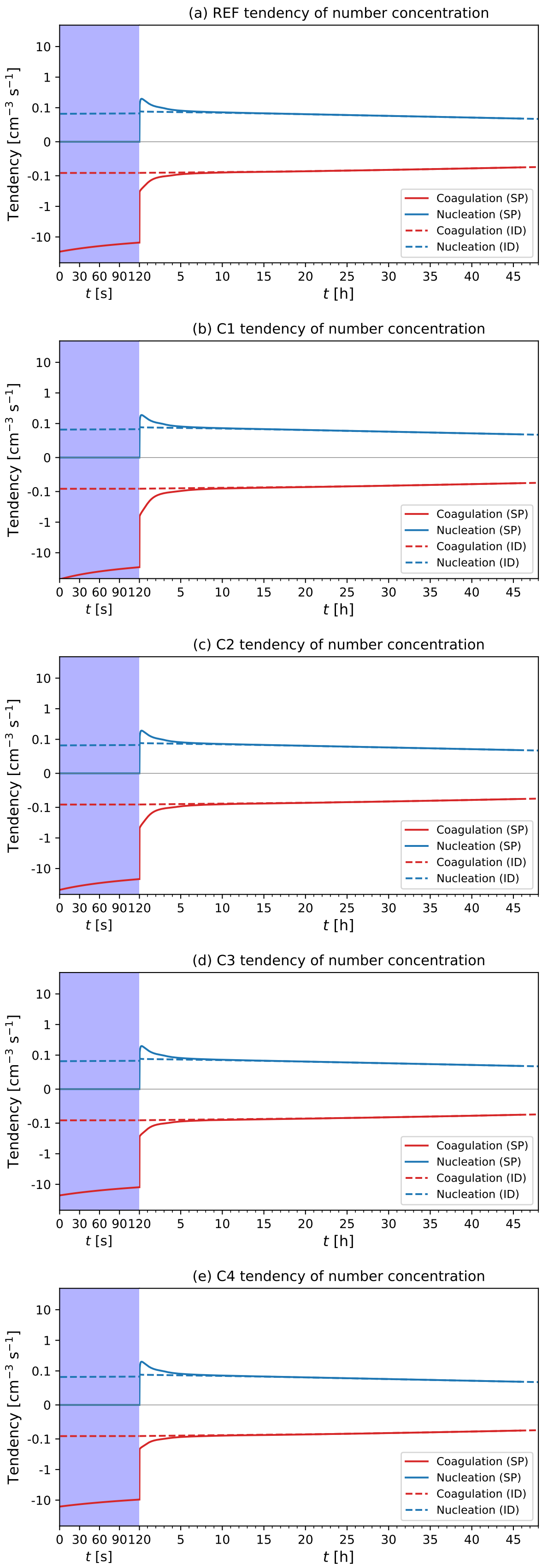

Figure S9: Tendency diagnostics as in Fig. S7, but for the parametric study C, demonstrating the modifications in the microphysical processes in response to altering the initial SO_4 size.

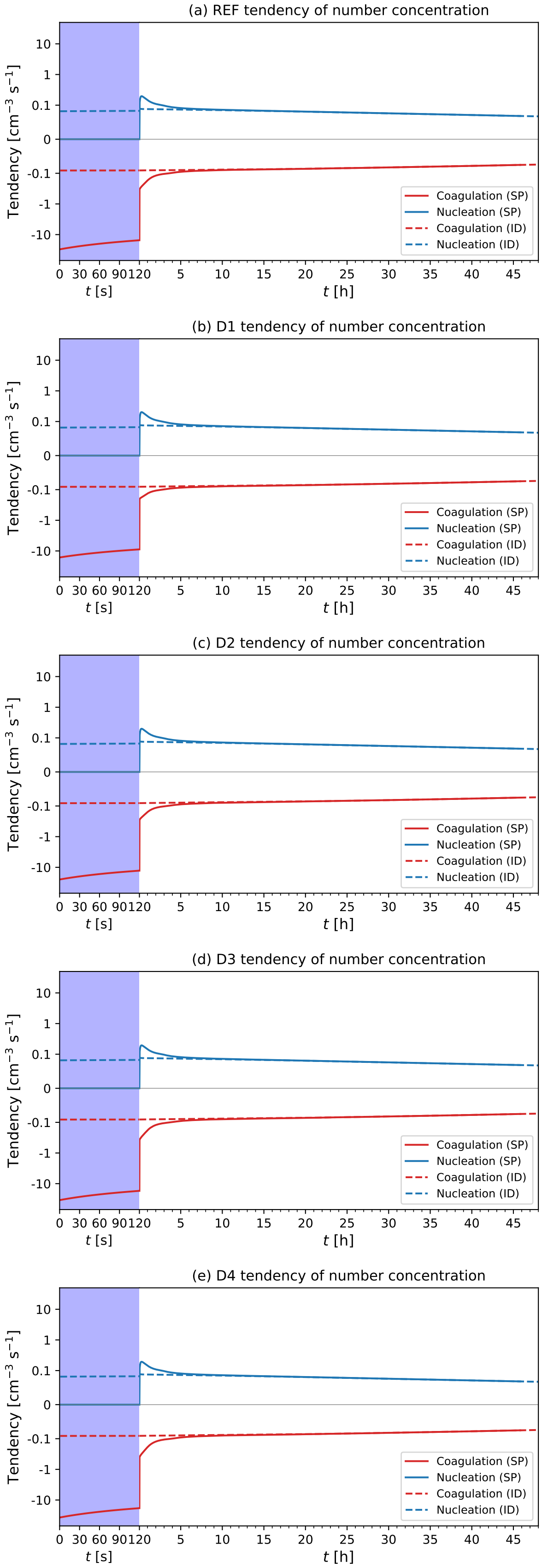

Figure S10: Tendency diagnostics as in Fig. S7, but for the parametric study D, demonstrating the modifications in the microphysical processes in response to altering the primary SO_4 values.

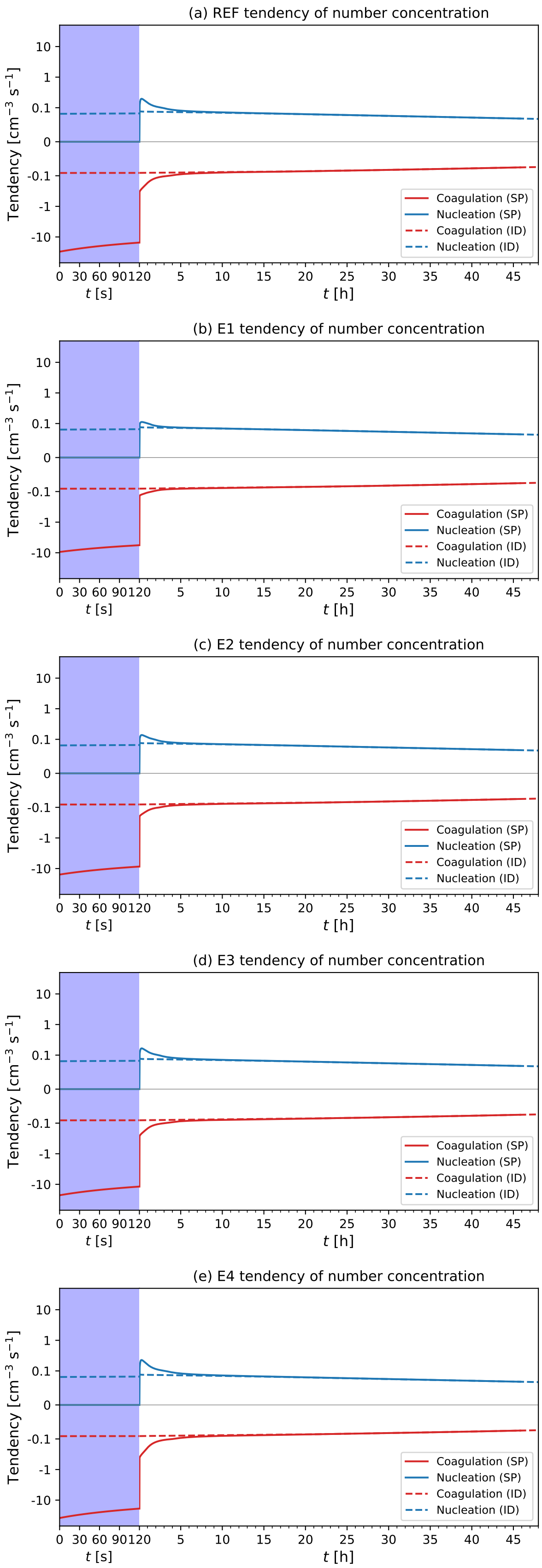

Figure S11: Tendency diagnostics as in Fig. S7, but for the parametric study E, demonstrating the modifications in the microphysical processes in response to altering the fuel sulphur content (EI_{SO_2}) values.

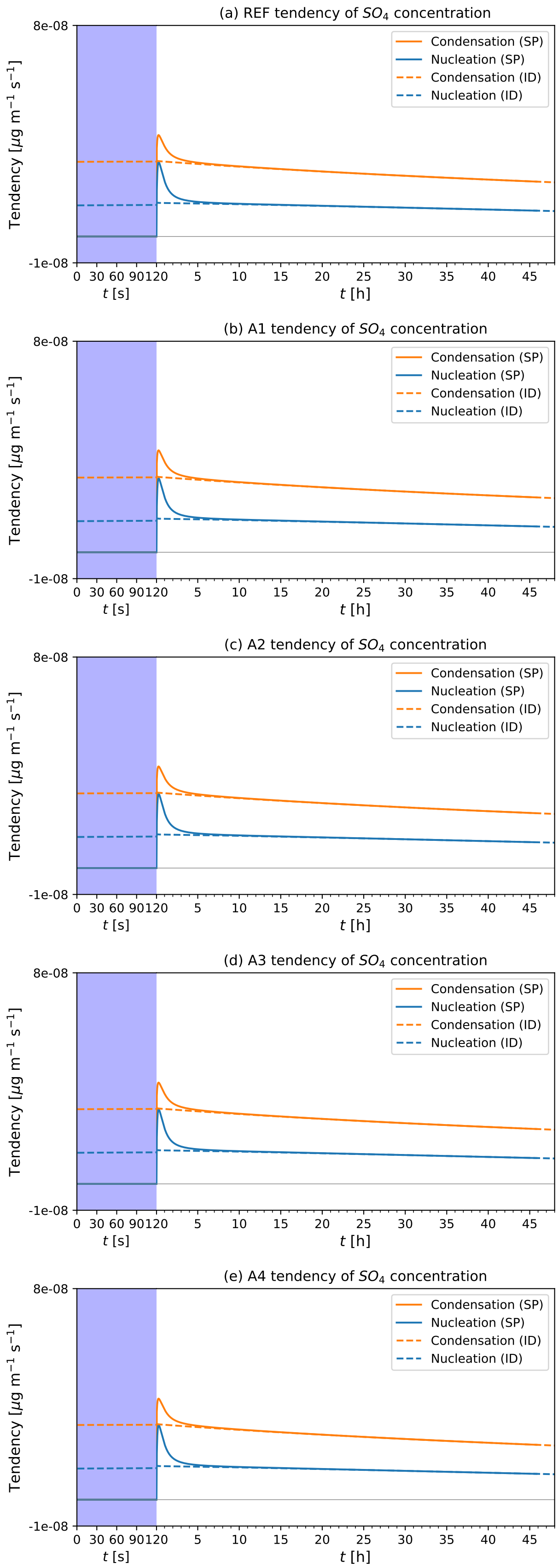

Figure S12: Tendency diagnostics as in Fig. S4, but for the parametric study A, demonstrating the modifications in the microphysical processes that influence the SO_4 mass concentration in the plume model i.e. condensation (orange) and nucleation (blue).

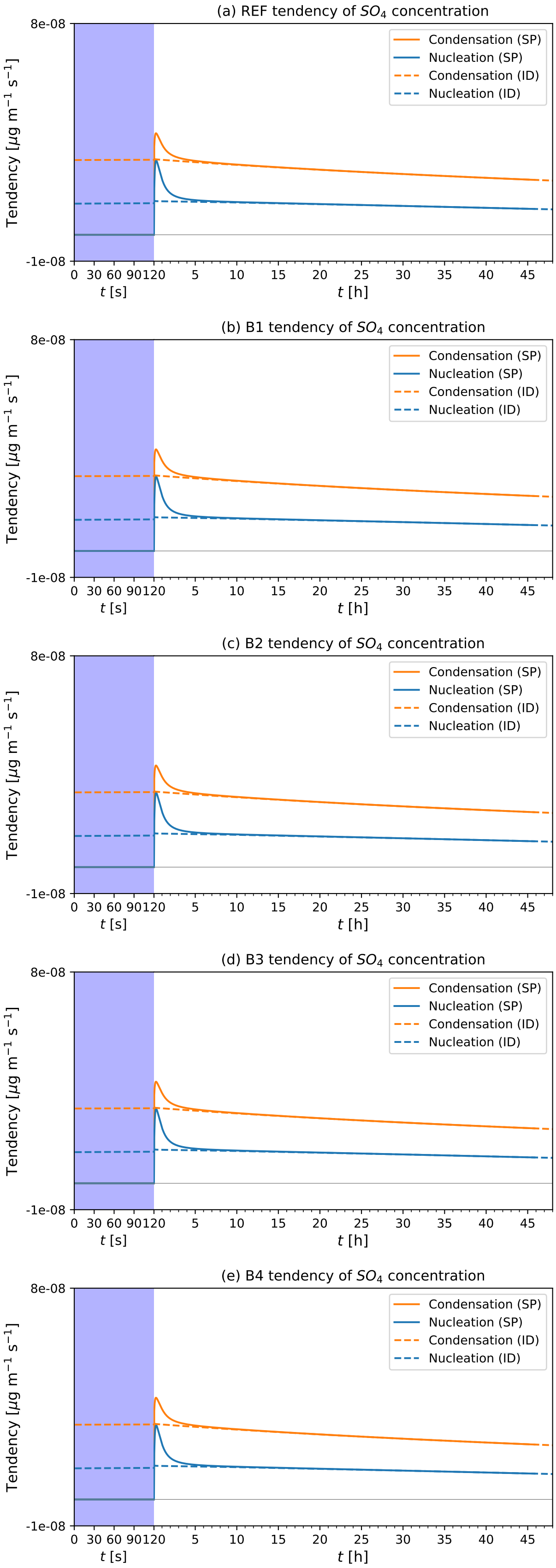

Figure S13: Tendency diagnostics as in Fig. S12, but for the parametric study B.

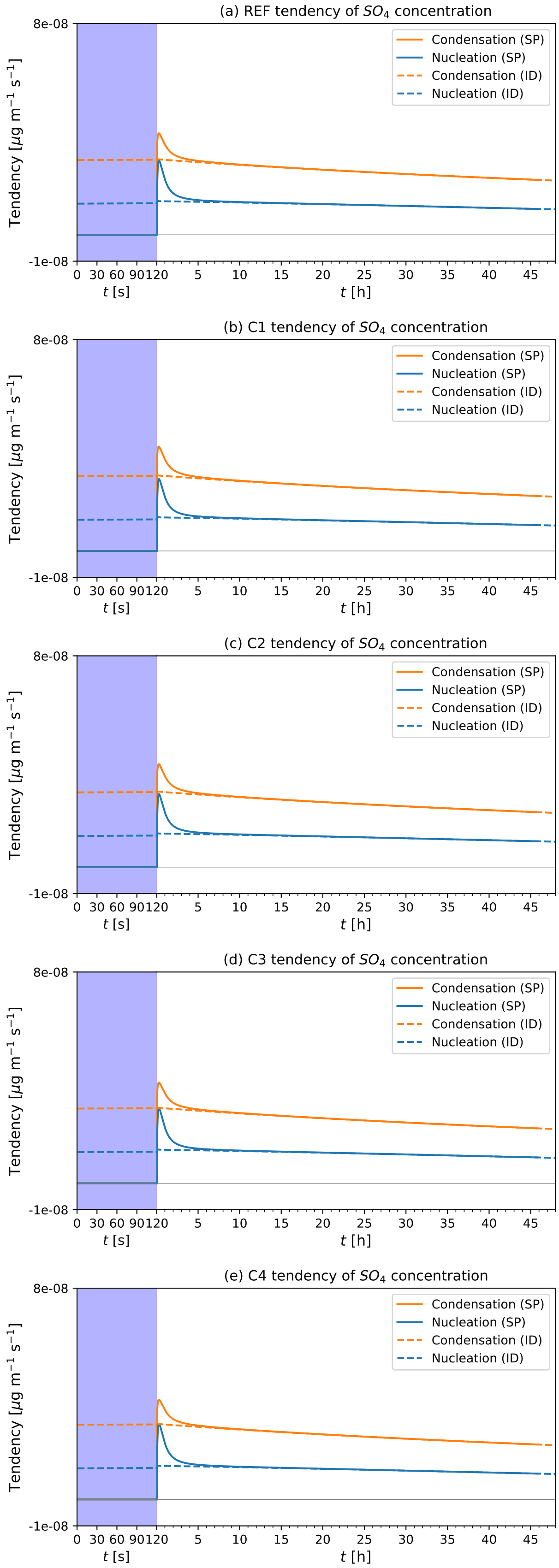

Figure S14: Tendency diagnostics as in Fig. S12, but for the parametric study C.

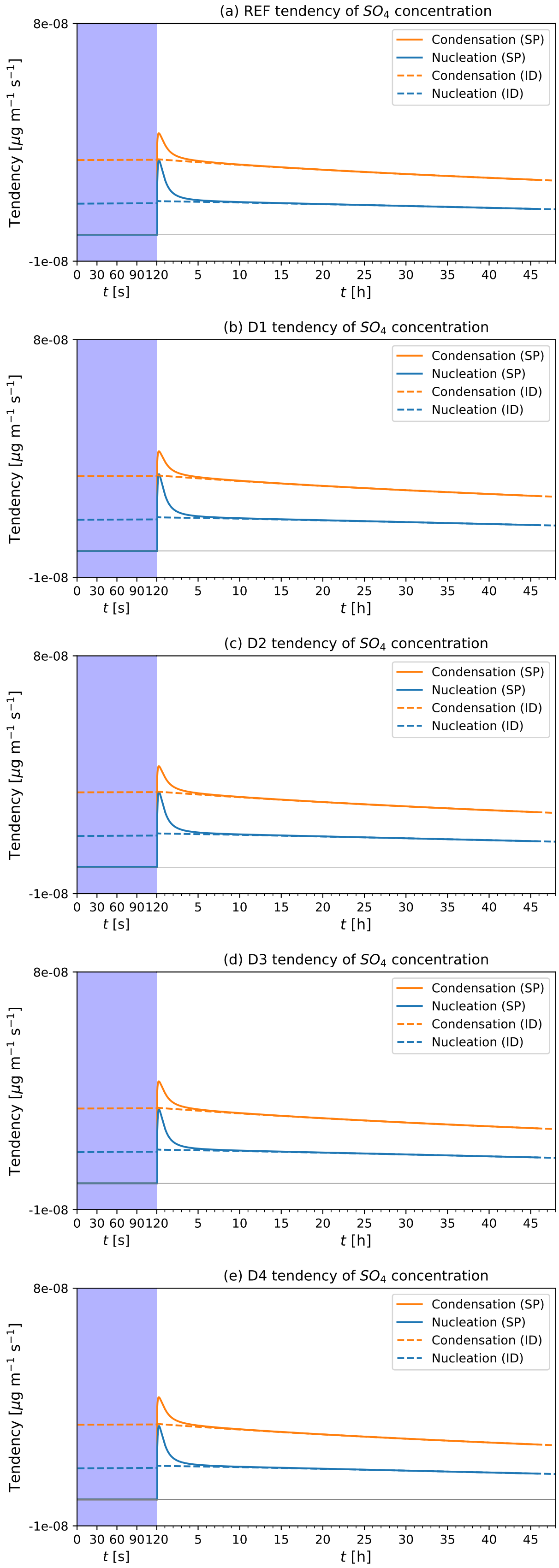

Figure S15: Tendency diagnostics as in Fig. S12, but for the parametric study D.

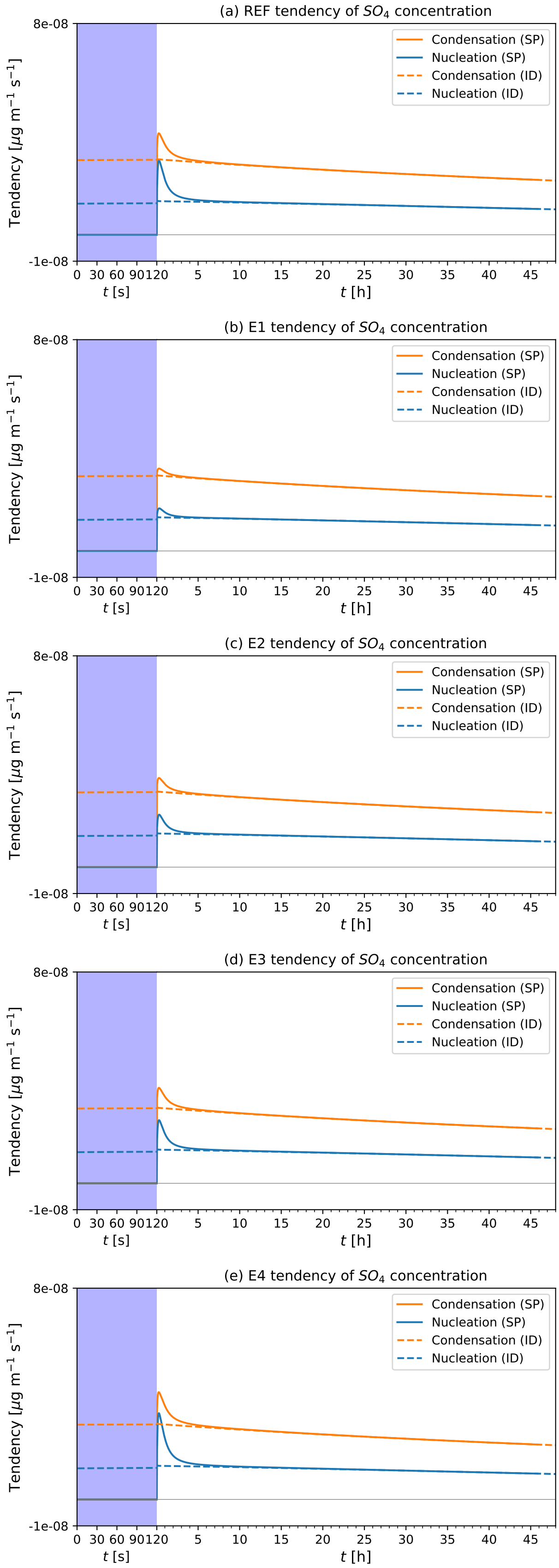

Figure S16: Tendency diagnostics as in Fig. S12, but for the parametric study E.